

# Super austenitic stainless steels – a promising replacement for the currently used type 316L stainless steel as the construction material for flue-gas desulphurization plant

N. RAJENDRAN, S. RAJESWARI

*Department of Analytical Chemistry, University of Madras, Guindy Campus, Madras 600 025, India*

Potentiodynamic anodic cyclic polarization experiments on type 316L stainless steel and 6Mo super-austenitic stainless steels were carried out in simulated flue-gas desulphurization (FGD) environment in order to assess the localized corrosion resistance. The pitting corrosion resistance was higher in the case of the super austenitic stainless steel containing 6Mo and a higher amount of nitrogen. The pit-protection potential of these alloys was more noble than the corrosion potential, indicating the higher repassivation tendency of actively growing pits in these alloys. The accelerated leaching study conducted for the above alloys showed that the super austenitic stainless steels have a little tendency for leaching of metal ions such as iron, chromium and nickel at different impressed potentials. This may be due to surface segregation of nitrogen as CrN, which would, in turn, enrich a chromium and molybdenum mixed oxide film and thus impedes the release of metal ions. The present study indicates that the 6Mo super austenitics can be adopted as a promising replacement for the currently used type 316L stainless steel as the construction material for FGD plants.

## 1. Introduction

The emission of SO<sub>2</sub>, a dangerous atmospheric pollutant, is the major problem with increasing use of coal as a fuel in various industries, particularly in thermal power plants. A variety of methods to minimize the SO<sub>2</sub> emission were reported in the literature among which the desulphurization of the flue gas generated by combustion of the coal has received much attention; this is termed flue-gas desulphurization (FGD). FGD scrubbers have found widespread use in thermal power plants, smelters, incinerators, and various refining operations [1–6]. Literature reports have shown that the capital cost incurred in installing an FGD system, amounts to almost 25% of the total cost of installation of whole thermal power plant. Hence adequate care should be taken in maintaining the plant from degradation of the materials due to corrosion and other related phenomena. It is very clear that the prevention of such a degradation is not only desirable but also mandatory.

However, the materials of construction used for FGD systems, usually type 316L stainless steel, have been reported to have failed due to the localized corrosion, namely, pitting and crevice corrosion attack, which can be induced by the aggressiveness of the environment, mainly of chloride, fluoride, acidity and temperature, encountered during the scrubbing of SO<sub>2</sub> [7–9]. It has been cited in the literature that the

pit could act as initiation and propagation sites for fatigue and stress corrosion cracking (SCC) failures [10–12]. At this juncture, there is a need to improve the corrosion performance of the currently used construction materials. This can be achieved by modifying the existing material by alloying with suitable elements.

In the present study, localized corrosion behaviour was studied on previously untried super austenitic stainless steels (alloy 31 and alloy 926, a product of VDM Corporation Limited) by means of electrochemical methods. The pitting corrosion resistance at various temperatures was evaluated and the performance in accelerated leaching under simulated FGD systems was assessed.

## 2. Experimental procedure

### 2.1. Electrode preparation

The chemical compositions of the super austenitics (alloys 31 and 926) and 316L stainless steels are given in Table I. Sheet materials in the as-received condition, were cut into 1 × 1 × 0.3 cm<sup>3</sup> size pieces for electrochemical studies. Measurement of current density was simplified by using these unit-area specimens. These specimens, attached to a brass rod for electrical connection, were mounted in an epoxy-based resin in such a way that only one side with 1 cm<sup>2</sup> surface area

TABLE I Chemical composition of the alloys (wt %)

Alloys	Cr	Ni	Mo	N	C	Fe	Others
316L	17.2	12.7	2.4	0.02	0.03	66	Mn, S
926	21	25	6.5	0.20	0.03	46	Cu, Mn, S
31	27	31	6.5	0.20	0.03	31	Cu, Mn, S

was exposed, and this formed the working electrode. In order to avoid the need for severe polishing after the resin mounting (which might cause micro-cracking at the metal-resin interface), the specimens were wet ground with SiC papers down to 800 grit followed by 5  $\mu\text{m}$  diamond paste. The electrodes were then ultrasonically cleaned in acetone and thoroughly washed in distilled water and dried.

## 2.2. Electrochemical cell assembly

The electrochemical cell consists of three compartments with a capacity of 500 ml. A saturated calomel electrode (SCE) was used as the reference electrode, platinum foil as the counter electrode and the specimen as the working electrode. The electrolyte used was a solution containing chloride, fluoride and sulphite, and the simulated FGD environment, the composition and operating conditions of which were as follows.

### Chemical composition

Chloride 10000 p.p.m.

Fluoride 1000 p.p.m.

Sulphite 2000 p.p.m.

### Operating conditions

pH 5.0

Temperature  $52 \pm 2^\circ\text{C}$

The pH of the electrolyte was adjusted with sulphuric acid. The working electrode was then introduced into the cell and the potential was allowed to stabilize for 15 min.

## 2.3. Polarization study

In the cyclic potentiodynamic polarization study, the potential was increased from rest potential in the noble direction at a rate of  $1\text{ mV s}^{-1}$  until the breakdown,  $E_b$ , was attained where the alloy entered the transpassive or pitting region. The sweep direction was then reversed after reaching an anodic current density of  $1\text{ mA cm}^{-2}$  until the potential where the reverse scan current density equals the upscan current density. The potential at which the reverse anodic scan meets the passive region is termed the pit-protection potential,  $E_p$ . The pitting potential of the above alloys were determined at various temperature ranges (room temperature, 50 and  $80^\circ\text{C}$ ).

The parameters of interest that were recorded during the polarization studies were (i) the corrosion potential,  $E_{\text{corr}}$ , (ii) the pitting potential,  $E_b$ , (iii) the pit-protection potential,  $E_p$ , and (iv) the safe region for corrosion attack,  $\Delta E$ .

## 2.4. Accelerated leaching of iron, chromium and nickel

In the accelerated leaching study, the working electrodes were immersed in the simulated FGD environment and allowed to stabilize at potentials of +100, 200, 300, 500 and at  $E_b$  for 1 h in 100 ml test solution. At the end of each experiment, the chemical composition of the test solution was analysed by inductively coupled plasma atomic emission spectrometry.

## 3. Results and discussion

### 3.1. Critical pitting potential

The corrosion potentials,  $E_{\text{corr}}$ , of alloys 31 and 926 were  $-340$  and  $-415$  mV, respectively, whereas type 316L stainless steel exhibited an  $E_{\text{corr}}$  at  $-475$  mV. The possible reason for the higher corrosion potential for super austenitic alloys is the presence of higher amounts of passivating elements, namely nitrogen, molybdenum and chromium.

The pitting potential is considered to be the criterion for evaluating the pitting corrosion resistance of the materials. The pitting potential of the alloy is directly influenced by the amount of passivating elements present in the alloy. A higher pitting corrosion resistance of the construction materials can be obtained by increasing the pitting potential of the alloy in the noble direction.

The critical pitting potentials for the super austenitic stainless steels (alloys 31 and 926) and type 316L stainless steel were determined from the anodic cyclic polarization curves, and they are shown in Fig. 1. The mean value of critical pitting potential for the type 316L stainless steel was  $+240$  mV. The presence of 0.2% nitrogen, 6% molybdenum and 21% chromium increased the  $E_b$  value to  $+850$  mV for alloy 926, whereas the presence of 6% Cr higher than in alloy 926 increased the  $E_b$  value to  $+875$  mV for alloy 31. Thus, it is evident that the austenitic stainless steels with higher nitrogen, chromium and molybdenum exhibited increased  $E_b$  value and they improved the pitting corrosion resistance under aggressive FGD environments.

Several studies have indicated that the addition of small amounts of nitrogen can lead to an improvement in pitting and passivation characteristics. Truman *et al.* [13] reported a remarkable increase in pitting corrosion of austenitic stainless steel owing to the addition of more than 0.25 wt % nitrogen. The addition of small amounts of nitrogen to the weld, wrought and austenitic stainless steel, improved their pitting corrosion resistance, sensitization resistance and mechanical properties. A synergistic influence of nitrogen and molybdenum on the pitting corrosion resistance was reported by Truman *et al.* [13] and Sedriks [14]. Newman *et al.* [15] noticed an enrichment of molybdenum and nitrogen in the passive film/metal interface and the enrichment of nitrogen was at least seven times the original concentration of nitrogen present in the alloy. They interpreted this enrichment of nitrogen and molybdenum at the interface as the predominant factor for preventing further

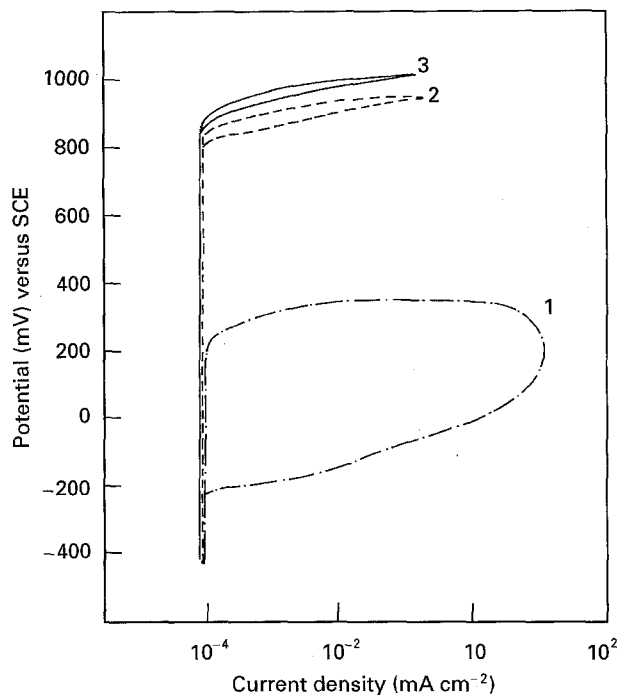


Figure 1 Potentiodynamic anodic polarization curves for (1) 316L SS, (2) alloy 926, and (3) alloy 31, in the simulated FGD environment.

dissolution of substrate consequent to the destruction of the passive film.

The increased pitting resistance of alloys 31 and 926 (both contain 2000 p.p.m. nitrogen) can be explained based on postulations of the previous workers. If the pit grows in the austenitic phase, the conditions prevailing at that pit site have been reported to be similar to those of the active dissolution state. Generally, during active dissolution, chromium and nickel dissolve, whereas non-active elements, such as nitrogen, can enrich at such a surface. Clayton and Martin [16] reported that nitrogen had a greater effect on improving the pitting resistance in the more acidic  $\text{SO}_4^{2-}/\text{Cl}^-$  solutions. From XPS studies they concluded that a significant amount of surface nitride was converted to  $\text{NH}_4^+$  ions, because  $\text{SO}_4^{2-}$  ions combined readily with  $\text{NH}_4^+$  ions and a pre-passive film was generated.

The nitrogen may be enriched in the surface of the passive films in stainless steels and it will inhibit anodic dissolution of the alloy by two orders of magnitude, presumably through the formation of source iron nitrides. This will certainly inhibit the auto-catalytic process of pitting formation and increase the opportunity for any pit to heal.

The morphology of the pitting attack observed from scanning electron microscopy on the above stainless steels is shown in Fig. 2a-c. The 316L stainless steel exhibits individually larger (roughly hemispherical) and deeper pits over the entire surface area of the specimen, as shown in Fig. 2a. This indicates a higher susceptibility of the material towards pitting attack.

The increase of passivating elements such as nitrogen, chromium and molybdenum in alloy 31 (Fig. 2b) showed lesser and smaller pits on those surfaces than

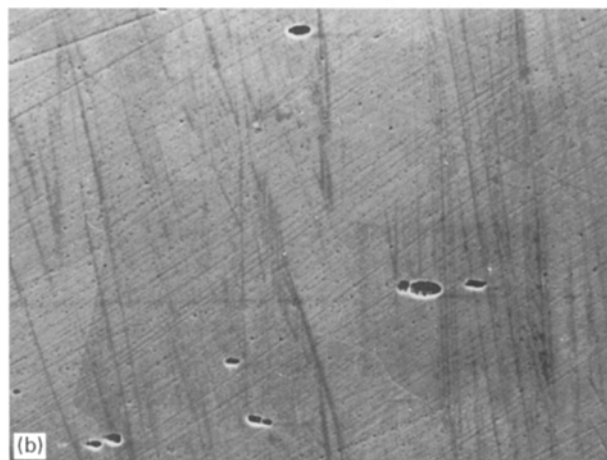
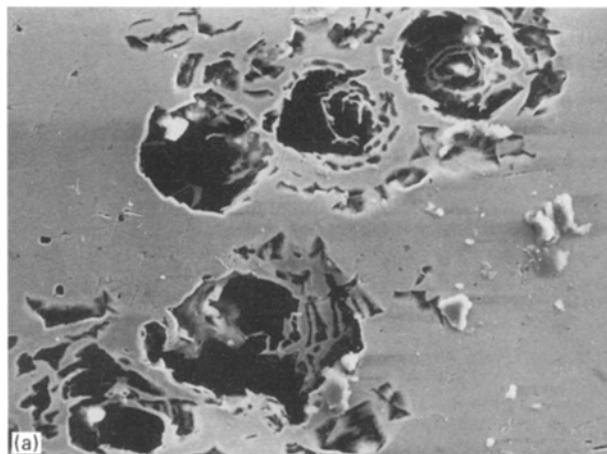


Figure 2 Scanning electron micrograph after the breakdown of the passive film for (a) 316 SS, (b) alloy 926, and (c) alloy 31, in the simulated FGD environment.

the reference type 316L stainless steel. The geometry of the individual pits observed was smaller and less pronounced when compared with type 316L stainless steel. Even though the enhanced pitting potential provided higher activation energy for the dissolution of alloy with the pit, it showed only feeble pitting attack. This indicated the promising role of higher amounts of passivating elements, namely nitrogen, chromium and molybdenum. An almost identical pitting behaviour was observed with alloy 926 (Fig. 2c).

### 3.2. Pit-protection behaviour

The pit-protection potential,  $E_p$ , was determined for the above alloys from the polarization curves (Fig. 1). The mean value of the pit-protection potential for type 316L stainless steel increased from  $-210$  mV to  $820$  mV owing to the addition of higher amounts of nitrogen (0.2%), molybdenum (6%) and chromium (21%), for alloy 926, whereas the addition of 6% higher chromium to alloy 926 increases the  $E_p$  value from  $-210$  mV to  $848$  mV. The significance of these observations is that new pits cannot be initiated above this potential, and hence it can be inferred that the increased nitrogen and molybdenum hinders the development of new pits and also slowed down the kinetics of growing pits.

The significant role of nitrogen in the pit-protection potential can be explained by the following facts. Once the passive film is damaged, the formation of a pit commences on the metal surface. If the pit grows, the conditions prevailing at that pit site have been reported to be similar to that of the active dissolution stage. In general, during active dissolution, the alloying elements, such as iron, chromium, and nickel dissolve, whereas non-active elements, such as nitrogen, can become enriched at the surface. Palit *et al.* [17] reported that the nitrogen was observed to be enriched significantly on the pitted surface, where its concentration was about 50 times higher than in the surrounding passive film or base-metal composition. The enrichment was maintained apparently to a great depth in the metal substrate. The formation of  $\text{NH}_3$  and  $\text{NH}_4^+$  following the reaction of surface nitrides with protons generated by metal hydrolysis, or from the bulk electrolyte, is a significant step by which the pH at the site is raised. This has the beneficial effect of aiding repassivation and stabilizing the passive film. This may provide an inactive layer to improve the pitting corrosion resistance.

The difference between pit-protection potential and corrosion potential for a given system is defined as the relative corrosion resistance,  $\Delta E$ . This value can be used to rank the alloys [11, 12]. The mean value of  $\Delta E$  for 316L stainless steel was  $225$  mV. The presence of nitrogen and molybdenum in this stainless steel increased the  $E$  value to  $1226$  mV, whereas for alloy 31,  $\Delta E$  increased to  $1251$  mV. A higher value of  $\Delta E$  reflects an enhanced resistance to pitting or accelerated general corrosion.

### 3.3. Accelerated leaching in a simulated FGD environment

In the accelerated leaching study, the concentrations of metal ions, namely iron, nickel and chromium, present in the test solution after ageing for 1 h were determined, and the results are illustrated in Figs 3–5. It is seen that significant amount of metal ions were released into the solution, even in the passive region, for type 316L stainless steel and the pitting attack occurred at  $+240$  mV, and hence the leaching study was not conducted at  $+300$ ,  $+500$  mV. Normally, the leaching of the metal ions from the construction

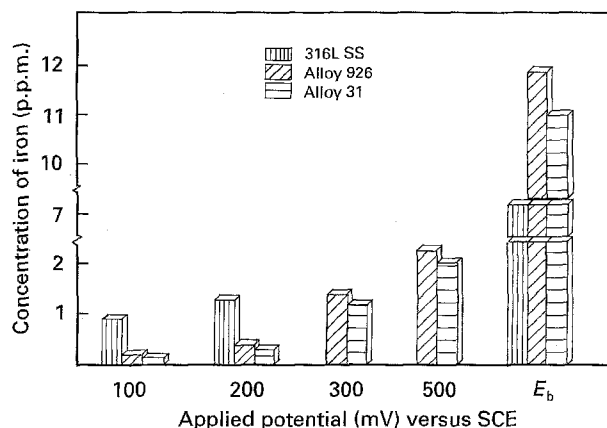


Figure 3 Concentration of iron present in the solution after the accelerated leaching of 316L SS, alloy 926 and alloy 31 at different imposed electrode potentials.

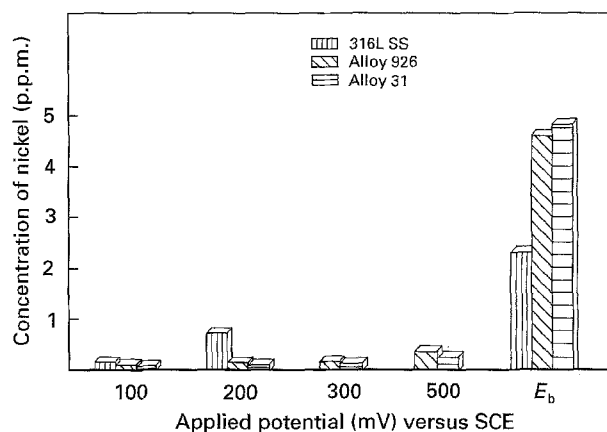


Figure 4 Concentration of nickel present in the solution after the accelerated leaching of 316L SS, alloy 926 and alloy 31 at different imposed electrode potentials.

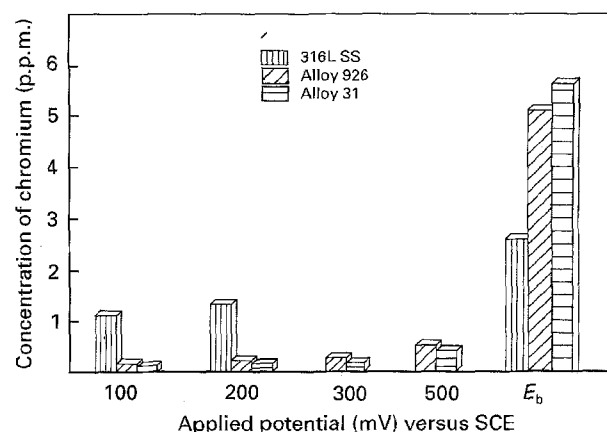


Figure 5 Concentration of chromium present in the solution after the accelerated leaching of 316L SS, alloy 926 and alloy 31 at different imposed electrode potentials.

material involves the adsorption of aggressive halide ions at the discrete sites on a passive metal surface as the first step. This process results in continuous thinning of the passive film until the bare metal surface is reached at the end of the induction period. Kruger [18] and Hoar and Jacob [19] have suggested the

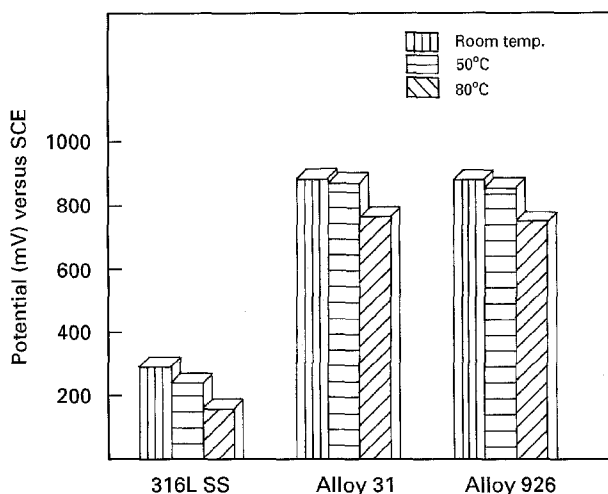


Figure 6 The temperature dependence of pitting potential in the simulated FGD environment.

formation of a transitional complex by the adsorption of three or four halide ions on the surface of the passive film around a lattice cation. Once the complex is formed, it readily removes the cation from the passive film lattice as a soluble species. Thus, thinning of the film occurs at the site where complex is formed, resulting in a stronger anodic field. This field rapidly pulls another cation through the thinned site of the film during the course of its interaction with halide ions. This again results in a soluble complex formation. The traverse of cations of the passive film is thus facilitated until the bare metal is reached.

In the present study, alloys 31 and 926 showed very little tendency for the leaching of metal ions compared to type 316L stainless steel at impressed potentials of +100, +200, +300, +500 mV. In these cases, the presence of higher nitrogen and molybdenum content may enrich the passive film interface and such enrichment could have strengthened the interface and impeded the release of metal ions through the passive film [20]. However, at the pitting potential, alloys 31 and 926 showed an enhanced leaching of iron, chromium and nickel. At the pitting potential, the increasing order of leaching of the metal ions was found to follow the order: 316L SS < alloy 926 < alloy 31. Nitrogen in these alloys improves the passive film, and a higher potential is required to initiate pitting compared to the 316L SS. Therefore, the relatively high potential at which pitting occurs may cause the pit to grow faster, and hence the release of metal ions was high in the alloys 31 and 926 at the higher pitting potential.

### 3.4. Effect of temperature

Fig. 6 shows the effect of temperature on pitting potential of alloys 31 and 926. It is evident that super austenitics showed a high resistance to pitting attack over a wide range of temperatures, whereas type 316L stainless steel showed a low corrosion resistance at all temperatures studied, particularly at 80°C. Agarwal and Heubner [21] noticed that high chromium- and molybdenum-containing alloys significantly improved the corrosion resistance and also at higher thermal conditions.

## 4. Conclusions

1. The critical pitting and pit-protection potentials of super austenitic stainless steels were more noble than those of the presently used type 316L stainless steel. This indicated the beneficial effect of nitrogen and molybdenum in improving the pitting resistance of austenitic stainless steels.

2. The accelerated leaching study indicated that the release of iron, chromium and nickel from the super austenitic stainless steel was considerably less compared to the type 316L stainless steel.

3. The pitting potential of super austenitic stainless steels in a simulated FGD environment is maintained over a wide temperature range.

## Acknowledgements

The authors thank VDM Corporation, Texas, USA, for providing the samples. The authors also thank Dr M. Vijayalakshmi, Scientific Officer, Metallurgy Division, IGCAR, Kalpakkam, India for providing the facilities to carry out SEM studies. The financial support extended by the Council of Scientific and Industrial Research (CSIR), New Delhi, India is gratefully acknowledged.

## References

1. A. I. ASPHAHANI, A. F. NICHOLAS, W. L. SILENCE and T. H. MAYOR, *Werkstoffe Korr.* **40** (1989) 409.
2. D. B. ANDERSON, in "Corrosion/81" (NACE, Houston, 1981) p. 13.
3. R. ROTH, *Werkstoffe Korr.* **43** (1993) 275.
4. R. R. SKABO, in "Proceedings of the Conference on Solving Corrosion problems in Air Pollution Control Equipment" (NACE, Houston, 1981) Paper 2.
5. M. X. CERNEY, *Corr. Rev.* **8** (1988) 60.
6. G. O. DAVIS, in "Corrosion/87" (NACE, Houston, 1987) Paper 456.
7. J. NAVETKSHI, *Power* **122** (1978) 72.
8. C. S. YOUUNG, in "Titanium for Energy and Industrial Applications", edited by D. Eylon (TMS-AIME, Warrendale, PA, 1981) p. 323.
9. N. RAJENDRAN, K. RAVICHANDRAN and S. RAJESWARI, *Bull. Electrochem.* **9** (1) (1993) 4.
10. M. SIVAKUMAR, U. KAMACHI MUDALI and S. RAJESWARI, *Steel Res.* **65** (2) (1994) 79.
11. M. SIVAKUMAR, U. KAMACHI MUDALI and S. RAJESWARI, *J. Mater. Sci. Lett.* **13** (1993) 142.
12. M. SIVAKUMAR and S. RAJESWARI, *ibid.* (1992) 1039.
13. J. E. TRUMAN, M. J. COLEMAN and K. R. PIRF, *Br. Corr. J.* **12** (1977) 236.
14. A. J. SEDRICKS, *Int. Metal. Rev.* **28** (1983) 306.
15. R. C. NEWMAN, Y. C. LU, R. BANDY and C. R. CLAYTON, in "Proceedings of the Ninth International Congress on Metallic Corrosion", Vol. 1 (National Research Council, Toronto, 1984) p. 394.
16. C. R. CLAYTON and K. G. MARTIN, in "Proceedings of the International Conference of High Nitrogen Steels HNS 88" (Institute of Metals, Lille, France 1988) p. 256.
17. G. C. PALIT, V. KAIN and H. S. GADIYAR, *Corrosion* **49** (1993) 977.
18. J. KRUGER, *Int. Mater. Rev.* **33** (3) (1988) 113.
19. T. P. HOAR and W. R. JACOB, *Nature* **216** (1967) 1299.
20. A. SADOUGH VANNI, J. P. AUDOWARD and P. MARCUS, *Corr. Sci.* **36** (1994) 1825.
21. D. C. AGARWAL and U. HEUBNER, in "Proceedings of the 12th International Corrosion Congress" Vol. 3A (NACE, Houston, 1993) 1226.

Received 17 March 1995  
and accepted 13 June 1996